Transcriptional responses of *Solanum lycopersicum* to three distinct parasites reveal host hubs and networks underlying parasitic successes

Julia Truch[1]*†, Maëlle Jaouannet[1]*, Martine Da Rocha[1], Emmanuelle Kulhanek-Fontanille[1], Cyril Van Ghelder[1], Corinne Rancurel[1], Olivier Migliore[1], Arthur Péré[1], Stéphanie Jaubert[1], Christine Coustau[1], Eric Galiana[1] and Bruno Favery[1]†

* These authors contributed equally to the current study

† Corresponding authors (julia.truch@inrae.fr, bruno.favery@inrae.fr)

Affiliations

[1]Institut Sophia Agrobiotech, INRAE, Université Côte d'Azur, CNRS, 400 routes des Chappes, 06903, Sophia-Antipolis, France.

Abstract

Crops face attacks from a wide range of pathogens and pests that deploy various parasitic strategies. All aggressors must manipulate major plant functions, such as immune signaling, hormone pathways, metabolism, and development, to successfully establish themselves and complete their life cycle. Here, we compared the tomato plant's response to three evolutionary distant pathogens (nematodes, aphids and oomycetes) during compatible interactions using a transcriptomic approach. We identified differentially expressed genes and biological processes, and highlighted potential key host hubs associated with successful parasitism. By integrating recent published datasets, we refined our understanding of the global and tissue-specific mechanisms targeted during compatible interactions and, through co-expression analysis, identified clusters showing shared dysregulation patterns enriched in specific GO terms. Finally, model-to-crop translational analysis using the Arabidopsis interactome network, repositioned tomato candidates within larger interaction networks and emphasized the key positions occupied by some of them. Identifying these pivotal tomato targets is crucial to decipher processes underlying parasitism and, consequently, offers new opportunities to develop sustainable multi-pathogen control strategies.

Keywords

Comparative transcriptomic meta-analyses, tomato, hub, network, parasitism, plant pathogens, nematode, oomycete, aphid

Introduction

Plants are severely challenged by soil-borne and aerial pathogens that threaten crop production worldwide. Cultivated tomato (*Solanum lycopersicum*), the most important vegetable crop by total production and second by harvested area globally (FAOSTAT2022; https://www.fao.org/faostat/en/#home; 186 Mt/year; 5 M of ha of surface harvested), is grown across a wide range of climates and serves as a host for numerous pathogens, including oomycetes, nematodes, and insects. In resistant plants, early detection of the pathogen through

basal immunity (pathogen-associated molecular patterns PAMP-triggered immunity, PTI) or later through the effector-triggered immunity (ETI) modulates MAPK signaling, transcription factors (WRKY, ERF, MYB…), epigenetic modifications, hormone imbalance (salicylic acid, jasmonate, auxins…) leading to productions of reactive oxygen species, pathogenesis-related proteins and secondary metabolites (Campos et al., 2021). Thus, compatible interactions between host plants and parasites rely on the avoidance of plant immunity and the reprogramming of the host's metabolic activity (Jones & Dangl, 2006). Consequently, pathogens hijack plant resources for their own profit, ultimately leading to reduced plant growth, yield losses, and potentially premature plant death (Kong & Yang, 2023).

As endoparasites, oomycetes and root-knot nematodes (RKN) have mastered long-term interactions within the host roots (Blok et al., 2008; Kamoun et al., 2015). On one hand, zoospores of the oomycete *Phytophthora parasitica* encyst and adhere to the plant surface before penetrating intercellularly. In the roots, *P. parasitica* hyphae invaginate host cell membranes, form haustoria and secrete apoplastic molecules, effectors, that promote pathogen development (Attard et al., 2008). At 15 hours post- infection, *P. parasitica* uses appressoria to penetrate host roots during an initial biotrophic phase (Attard et al., 2010). On the other hand, the mobile infective second-stage juveniles of the RKN *Meloidogyne incognita* penetrate host roots, and migrate intercellularly until reaching the central cylinder, where they become sedentary and induce a feeding structure composed of several giant multinucleate cells. At 21 days post infection (dpi), giant cells are fully differentiated and function as mature, metabolically active feeding structures that sustain RKN development (Abad et al., 2008; Favery et al., 2020).

In contrast, aphids such as *Macrosiphum euphorbiae* are ectoparasites establishing durable yet transient interactions by feeding on host plants via sap-sucking (Walling, 2008). Aphid colonies develop on the leaf surface and winged adults ensure the dissemination of new colonies. At 24 hours post-infection in a confined space, aphids have induced their feeding and the host displays a peak response (Jaouannet et al., 2015). Similar to *M. incognita*, *M. euphorbiae* uses a stylet to deliver effectors that manipulate host immunity and metabolism, enabling nutrient acquisition and colony establishment (Favery et al., 2020; F. Wang et al., 2021).

Characterizing both the host targets of effectors and the host functions manipulated is essential to decipher the mechanisms underlying parasitic success, and represents a crucial step to develop new strategies to control pathogens. The diversity of life traits is associated with effector multiplicity which, overall, converges to target directly or indirectly fundamental host components. Interestingly, evolutionary distant pathogens deploy effectors that interact with the same host targets (Mukhtar et al., 2011; Carella et al., 2018). Such shared targets are often interconnected key molecules, hubs, whose perturbation can compromise the robustness of the host regulatory networks. In this context, monitoring plant transcriptional activity is a relevant approach to identify key factors and pathways commonly targeted by pathogens. Some independent works individually analyzed the transcriptomic response of *S. lycopersicum* to the parasites used in our study (i.e. *M. incognita*, *M. euphorbiae* and *P. parasitica*) (Coppola et al., 2013; Naveed & Ali, 2018; Mejias et al., 2021). However none of them investigated and integrated all the responses in a cordonnated experimental procedure and single analysis. Comparative transcriptome meta-analyses focusing on a single model plant or crop species exposed to multiple pathogens, are gaining momentum. These studies reanalyze public RNA-seq datasets to generate multi-pathogens plant response profiles (Biniaz et al., 2022; Y. Wang et al., 2022). Conversely to these studies, which rely on conditions defined by the original experiments, our study used the same tomato variety, matching the tomato reference genome for optimal mapping of RNA-seq data, plants grown under the same conditions and carefully chosen infection time points. To this end, we assessed the transcriptomic response of *S. lycopersicum var. 'Heinz 1706'* infected or not by the RKN *M. incognita*, the oomycete *P. parasitica* or the aphid *M. euphorbiae*, using comparative RNA-seq approaches and pathway analyses. Beyond the identification of genes that are strongly and commonly dysregulated upon infection, we

implemented a co-expression analysis to pinpoint candidate hubs associated with parasitic success and to position homologs of these candidate gene products within their interactome network environment.

Methods

Material production

Six four-week-old plants of *S. lycopersicum var. 'Heinz 1706'* per replicate were grown in a growth chamber under a 16-h photoperiod at 24°C and inoculated with 1000 J2s of *M. incognita* or 500,000 zoospores of *P. parasitica* in the soil, or 50 mixed stages *M. euphorbiae*. Root galls resulting from *M. incognita* infection were collected at 21 dpi, *P. parasitica*-infected roots were harvested 15 hpi, and leaves attacked by *M. euphorbiae* were sampled 24 hpi. For each condition, equivalent roots or leaves tissues were collected from non-infected plants. Four independent biological replicates were produced per condition.

RNA extraction

Samples were ground with mortars in liquid nitrogen and transferred to new tubes. Four volumes of extraction buffer (0.1 M Glycine-NaOH pH 9, 0.1 M NaCl, 0.1% SDS and 1% deoxycholic acid sodium salt) were added. Samples were incubated 5 min on ice, centrifuged for 5 min and supernatants were transferred to fresh tubes. One volume of phenol:chloroform:isoamyl alcohol (PCI; 25:24:1, v/v/v) was added. Samples were vortexed for 15 sec, incubated 2 min at room temperature and centrifuged at 15,000 × g for 15 min at 4°C. The aqueous phase was collected and a second extraction with PCI was performed. The aqueous phase was washed twice with one volume of chloroform before been centrifuged at 12,000 × g for 15 min at 4°C. Sodium acetate was added to a final concentration of 0.3 M, followed by one volume of cold 100% isopropanol. Samples were incubated overnight at -20°C and centrifuged at 12,000 × g for 15 min at 4°C. RNA pellets were washed twice with 1 ml of 70% ethanol, centrifuged at 12,000 × g for 5 min at 4°C, air dried for 10 min, resuspended in 100 µl of RNase free water and 33µl of 8M Lithium Chloride and incubated for one hour at -20°C and centrifuged at 12,000 × g for 5 min at 4°C. Pellets were washed twice with 1ml of cold 70% ethanol, air-dried 10 min and resuspended in 25 µl of RNase free water at 55°C for 5 min. gDNA contamination was removed using Qiagen RNeasy Plus kit following the manufacturer's instructions.

Library preparation and sequencing

Library preparation and sequencing were performed by Eurofins Genomics Europe Sequencing GmbH. RNA samples were assessed for integrity and quality and strand-specific, directional polyA selected library preparation was performed using NEBNext Ultra II Directional RNA Library Prep Kit for Illumina with TruSeq Adapter sequences. The samples were sequenced on Illumina NovaSeq 6000 platform using 2x150 Sequence mode.

Raw data analysis

Raw data were analyzed using an in-house Nextflow based pipeline. Briefly, quality controls of raw data were performed using FastQC (fastqc%3A0.11.9--hdfd78af_1) and MultiQC (multiqc%3A1.10.1--pyhdfd78af_1) before and after data cleaning including trimming and filtering for reads of at least 100 bp using FastP (fastp%3A0.23.2--h79da9fb_0). Reads were then mapped with STAR (star%3A2.7.8a--h9ee0642_1) with the options --genomeSAindexNbases 10 for the

128 indexing and --alignEndsType EndToEnd and --twopassMode Basic for the mapping. For each
129 interaction, reads were mapped on a composite genome combining *S. lycopersicum* v4 genome
130 (solgenomics.net) with either the *M. incognita* V3 genome (Blanc-Mathieu et al., 2017), the *M.*
131 *euphorbiae* transcriptome (NCBI ref GAOM01000000) or the *P. parasitica* genome
132 GCA_000247585.2 (https://protists.ensembl.org) in order to remove potential pathogen reads.
133 Then, all reads mapping to pathogen genome/transcriptome were removed to conserve only the
134 reads mapping to the *S. lycopersicum* v4 genome. Read counts were obtained with Feature-Counts
135 (subread:2.0.1--hed695b0_0) with the options -t mRNA and -g ID. Differential analyses were
136 performed using DESeq2 and EdgeR. The gene annotation was based on the *S. lycopersicum*
137 annotation ITAG4.1 (solgenomics.net). Principal component analysis (PCA), VENN diagrams and
138 co-expression analyses in roots and leaves were performed using DiCoExpress (Lambert et al.,
139 2020). Graphical representations were performed with ggplot2 (ggplot2_3.5.0). Filtering,
140 normalization and quality control (including PCA analysis) of the dataset were performed using the
141 Quality_Control option with default parameters (CPM_Cutoff=1 and Normalization_Method =
142 "TMM"). Datasets were analyzed using GLM_Contrasts model taking into account the interaction.
143 DiffAnalysis.edgeR was run with default parameters (Alpha_DiffAnalysis = 0.05, NbGenes_Profiles
144 = 20, NbGenes_Clustering = 50). Venn diagrams were performed using Venn_IntersectUnion
145 option. Co-expression analyses were performed using Coexpression_coseq option based on
146 Gaussian mixture models using default parameters on gene candidates commonly dysregulated in
147 roots or leaves pathogens therefore excluding the candidates present in the respective interactions.
148 Singularity prebuilt images were retrieved from the Galaxy Project Singularity Depot
149 (https://depot.galaxyproject.org/singularity/).

150 **Subtilase and TCP gene family analyses**

151 Fifty-five protein sequences were retrieved from TAIR (Araport11), matching with the 56 subtilases
152 described in A. Figueiredo et al. (2014), with AT3G44262 removed because it is a pseudogene).
153 Similarly, 103 protein sequences annotated as subtilase were extracted from the *S. lycopersicum*
154 protein dataset (ITAG4.1). The 158 sequences were aligned using MUSCLE (v3.8.31) with default
155 settings for highest accuracy. No outgroup has been added as the objective was to position *S.*
156 *lycopersicum* sequences according to *A. thaliana* sequences and the known subtilase sub-families.
157 The phylogenetic tree was reconstructed using the maximum likelihood method implemented in the
158 PhyML program (v3.1/3.0 aLRT). The WAG substitution model was selected assuming an
159 estimated proportion of invariant sites (of 0.000) and 4 gamma-distributed rate categories to
160 account for rate heterogeneity across sites. The gamma shape parameter was estimated directly
161 from the data (gamma=1.197). Reliability for internal branch was assessed using the aLRT test
162 (SH-Like). Graphical representation and edition of the phylogenetic tree were performed with iTOL
163 v7. Similarly, 24 and 32 protein sequences annotated as TCP transcription factors were retrieved
164 from the *A. thaliana* (Araport11) and the *S. lycopersicum* (ITAG4.1) protein datasets, respectively.
165 These 56 sequences were aligned with MEGA X using MUSCLE. The evolutionary history was
166 inferred using the Neighbor-Joining method. The bootstrap consensus tree was inferred from 1000
167 replicates. The evolutionary distances were computed using the JTT matrix-based method.

168 **Gene ontology (GO) and transcription factor analyses**

169 The GO analyses were performed with GOFuncR (GOfuncR_1.22.2) except the co-expression
170 analysis part for which the GO analyses were performed using DiCoExpress using Enrichment
171 option with default parameters (Alpha_Enrichment=0.01) (Lambert et al., 2020). Visualisation was
172 done with ggplot2 (3.5.0). The list of transcription factors was downloaded from the Plant

173 Transcription Factor Database (PlantTFDB v5.0) (https://planttfdb.gao-lab.org/index.php?sp=Sly)
174 (Tian et al., 2019).

175 **Ortholog identification, effector interactor and interactome network analyses**

176 Protein sequences from *S. lycopersicum* (ITAG4.1), *Arabidopsis thaliana* (Araport11), *Amborella*
177 *trichopoda* (AMTR1.0), *Brassica napus* (AST_PRJEB5043_v1), *Capsicum annuum*
178 (ASM51225v2), *Coffea arabica* (GCF_003713225.1_Cara_1.0), *Helianthus annuus* (HanXRQr2.0-
179 SUNRISE), *Medicago truncatula* (MedtrA17_4.0), *Nicotiana benthamiana* (Niben261), *Oryza sativa*
180 (IRGSP-1.0), *Prunus persica* (NCBIv2), *Sorghum bicolor* (NCBIv3), *Selaginella moellendorffii*
181 (v1.0), *Solanum tuberosum* (SolTub_3.0), *Vitis vinifera* (PN40024.v4) and *Zea mays* (Zm-B73-
182 REFERENCE-NAM-5.0) were functionally annotated using InterProScan (5.51-85.0) and the
183 ortholog analysis was performed using OrthoFinder (2.5.4). The identification of effectors
184 interacting with candidate homologs was performed using EffectorK (González-Fuente et al.,
185 2020). *A. thaliana* based interactome was generated with BIOGRID-ORGANISM (v4.4.227) using
186 BIOGRID-ORGANISM-Arabidopsis_thaliana_Columbia-4.4.227.psi25 and analysed with
187 Cytoscape (v3.10.1).

188 ## Results

189 **Global transcriptomic response of S. lycopersicum to M. incognita, P. parasitica and M.**
190 **euphorbiae**

191 We performed comparative RNA-seq analyses on *S. lycopersicum* roots inoculated or not with
192 either *M. incognita* or *P. parasitica* and leaves inoculated or not with *M. euphorbiae,* to assess the
193 transcriptional reprogramming occurring in tomato under biotic stresses. To be considered as
194 differentially expressed genes (DEGs), candidates had to display both, an adjusted p-value < 0.05
195 in DEseq2 analysis and FDR < 0.05 in EdgeR analysis. Thus, we identified 12,231 DEGs at 21 dpi
196 with *M. incognita*, 12,018 DEGs at 15 hpi with *P. parasitica* and 11,001 DEGs at 24 hpi with *M.*
197 *euphorbiae* (Figure 1a and Figure S1). Each interaction displayed a high number of DEGs with
198 similar proportions of up- and down-regulated candidates (Figure 1a). A total of 4,461 DEGs were
199 identified in response to the three pathogen infections (Figure 1b). Among them, 961 were down-
200 regulated and 645 were up-regulated across all three conditions, whereas 2,855 showed variable
201 dysregulation patterns depending on the specific interaction studied (Figure 1c). To obtain an
202 overview of the biological processes commonly targeted by the three pathogens, we performed GO
203 enrichment analyses on the lists of DEGs identified. We identified 53 biological processes GO
204 terms shared across the three interactions (Figure 1d). Among them, 45 GO terms were all either
205 over- or under-represented (Figure S2a), whereas eight showed variability depending on the
206 specific interaction (Figure S2b). All over-represented GO terms were related to metabolic
207 processes, while the negative regulation of metabolic processes were among the under-
208 represented GO terms. These results are consistent with the enhanced metabolic activity of the
209 host associated with pathogen infection.
210 Focusing on the DEGs most strongly responsive to all three pathogens, we identified only 11 genes
211 with a log2 fold change (log2FC) < -2 across all interactions (Figure 1e). This short list includes the
212 *TOLERANT TO CHILLING AND FREEZING 1* (*AtTCF1*) Arabidopsis ortholog, *Solyc05g052950.*
213 This stress response-associated gene encodes for a regulator of chromosome condensation that
214 indirectly affects lignin accumulation (Ji et al., 2015). Surprisingly, the list also contains two *A.*
215 *thaliana* orthologs of transcription factors that are involved in plant pigment regulation (flavonol and
216 chlorophyll, respectively): the *Solyc06g005330,* related to the AtMYB48 transcription factor and
217 *Solyc12g009240*, a putative ethylene-responsive transcription factor (homolog of ERF017 in *A.*

218 *thaliana*). Conversely, 10 DEGs displayed a log2FC >2 in three interactions (Figure 1f). Among
219 them, we identified genes that are involved in a variety of biological responses. Notably, we
220 identified tomato orthologs of *A. thaliana* proteins known to regulate systemic acquired resistance
221 (SAR), such as the NON-INDUCIBLE IMMUNITY1 (NIM1)-INTERACTING 2-like protein
222 (Solyc04g007140); proteins induced upon biotic stress, such as N-acetyltransferase NATA induced
223 by insect feeding and bacterial infection (Solyc08g006765) (Adio et al., 2011; Lou et al., 2016) or
224 abiotic stresses, such as the chromatin remodeling factor OXIDATIVE STRESS 3 (OXS3,
225 Solyc06g066420) (Blanvillain et al., 2009). Finally, we identified two susceptibility factors: (i) the
226 osmotin-like protein OSM34 (Solyc08g080670), which is subverted in *A. thaliana* by the turnip
227 mosaic virus (TuMV) thus decreases plasmodesmata callose deposition to promote viral cell-to-
228 cell movement and replication (He et al., 2025), and (ii) DOWNY MILDEW RESISTANT6 DMR6,
229 an enzyme that converts SA into its inactive form and whose loss of function in tomato confers
230 broad-spectrum disease resistance (Thomazella et al., 2021). Consistently, both *DMR6-1* and
231 *DRM6-2* (*Solyc03g080190* and *Solyc06g073080*) were upregulated in the three interactions tested
232 (Figure 1f and Figure S2c).

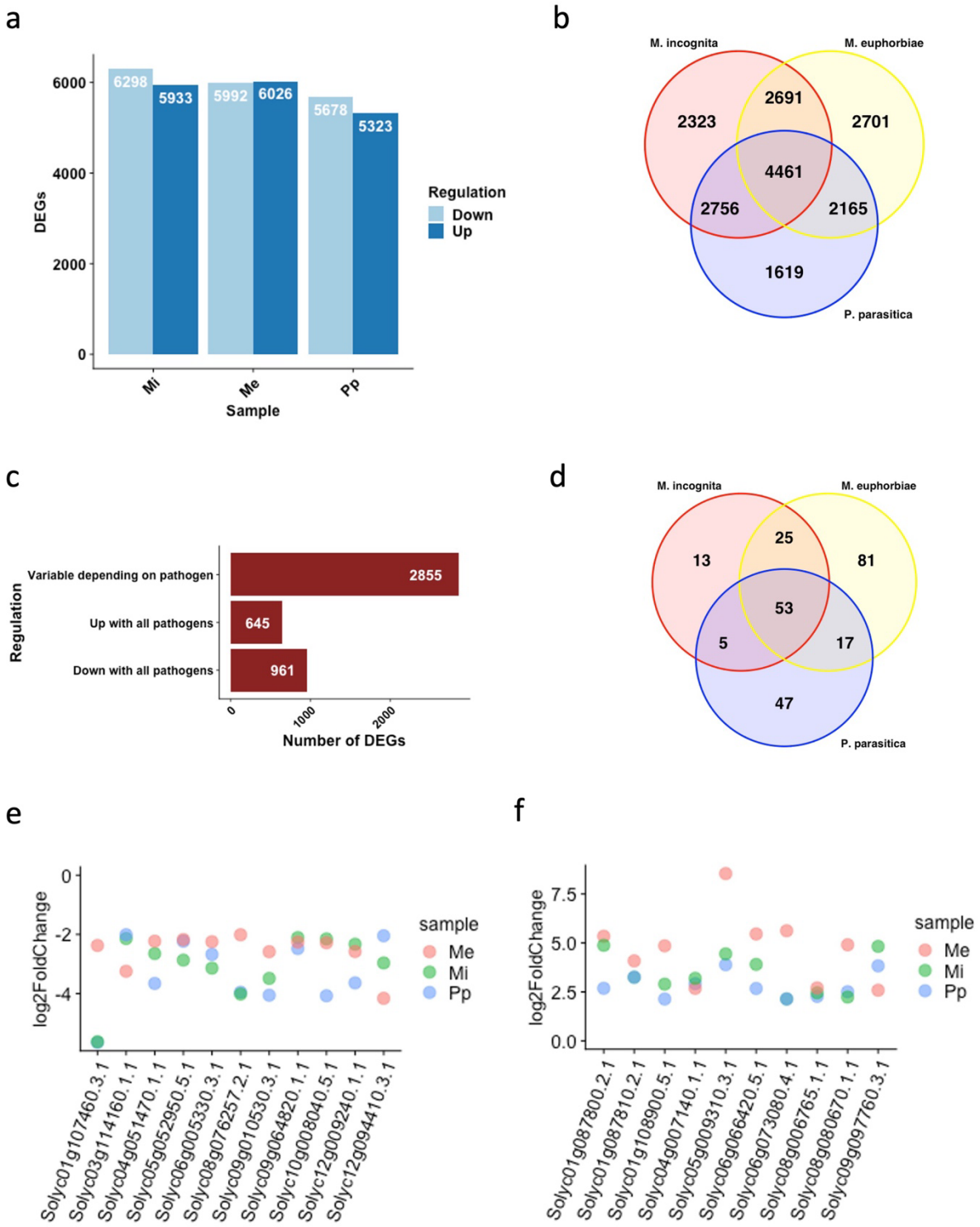

Figure 1 - Transcriptomic response of *S. lycopersicum* to *M. incognita*, *P. parasitica* and *M. euphorbiae*. a. Barplot showing the number of DEGs up- and down-regulated depending on the tested parasites. b. Venn diagram illustrating the overlap between the DEGs identified in the experiments with the different parasites. c. Barplot comparing the change in gene expression of the 4461 candidate genes differentially expressed during the three interactions. D. Venn Diagrams of GO overlap between the three interactions considering all the DEGs. e. DEGs with a log2FC < -2 in the three interactions tested. f. DEGs with a log2FC > 2 in the three interactions tested. Me: *M. euphorbiae*, Mi: *M. incognita* and Pp: *P. parasitica*.

243 Furthermore, we identified two subtilases (or subtilisin-like proteases) among the top 10 most
244 strongly upregulated DEGs in response to the three parasites. These two proteases encoding
245 genes (*Solyc01g087800* and *Solyc01g087810*) were arranged in tandem within a larger subtilase
246 cluster (cluster 1) on the chromosome 1 (Figure 2). The subtilase gene family was particularly well
247 represented in our DEG dataset. Indeed, 65 of the 103 annotated subtilase genes in tomato were
248 differentially expressed in response to at least one pathogen. A deeper focus on the subtilase
249 cluster 1 revealed additional subtilase candidates differentially expressed in each plant-parasites
250 interaction (Figure 2). The phylogenetic tree built with the subtilases of *A. thaliana* and *S.*
251 *lycopersicum* showed that subtilases from cluster 1 are all related to the *A. thaliana* gene *SBT1.9*
252 (*At5g67090*). In addition, the subtilase cluster 8, previously characterized in tomato (Reichardt et
253 al., 2018), also contained numerous pathogen-responsive genes (Figure 2). Interestingly, both
254 clusters included subtilases identified as phytaspases, caspases-like proteases regulating
255 programmed cell death, including *Solyc01g087800,* the most highly expressed candidate. Our
256 results showed that subtilases in Arabidopsis have more gene members from the subfamilies SBT3
257 and SBT4 than in tomato. Conversely, tomato subtilases undergo a massive expansion in the SBT1
258 subfamily that includes subtilases from the clusters 1 and 8 (Figure 2).

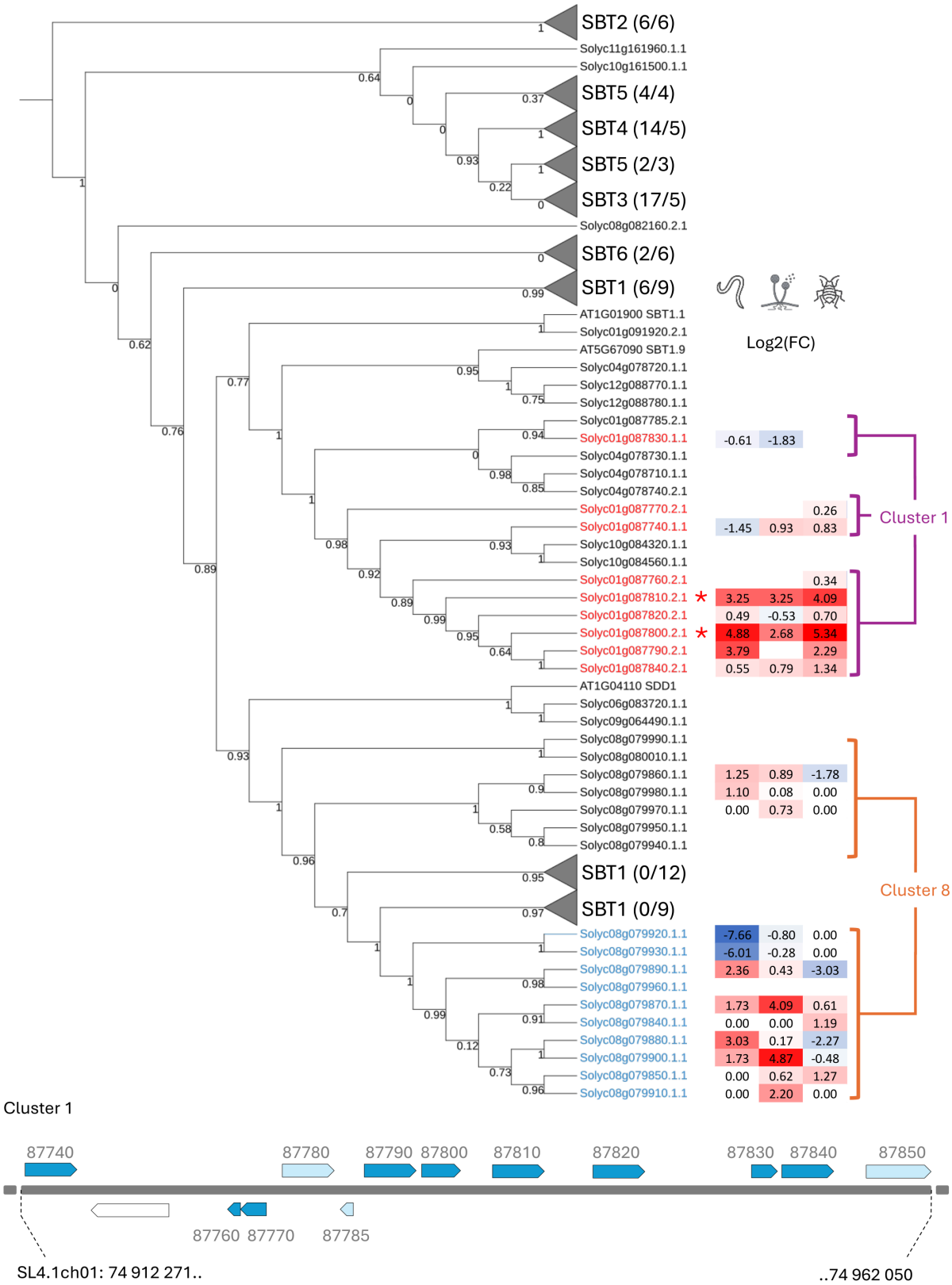

Figure 2 - Phylogenic tree of subtilases of the cluster 1 and 8 in the chromosome 1 and 8 of *S. lycopersicum*. The ML phylogenetic tree (WAG model, aLRT test) contains 55 subtilases from A. thaliana and 103 subtilases from *S. lycopersicum*. SBT1-6 subfamilies were assigned following (A. Figueiredo et al., 2014) and clades

were collapsed to facilitate the visualization (the extended developed phylogenetic tree is available in Figure S3). In brackets, the number of *A. thaliana* sequences/number of sequences from *S. lycopersicum*. The differential expression (Log2 Fold Change) of genes from the cluster 1 and 8 (from chromosome 1 and 8 of *S. lycopersicum*) in response to the three pathogens (*M. incognita*, *P. parasitica* and *M. euphorbiae*) is presented on the right panel. Asterisks indicate the two highly overexpressed genes in response to the three pathogens. Physical representations of the Cluster 1 and 8, including their coordinates on the *S. lycopersicum* chromosome 1 and 8, respectively, are presented with differentially expressed subtilase genes in response to at least one pathogen in dark blue and light blue for the others.

In-depth identification of targeted hubs during plant-pathogen interactions

Following the identification of the most strongly dysregulated genes, we next analyzed DEGs through the lens of common stress-response pathways. We first examined the salicylic acid (SA) pathway and, in addition to *DMR6s* and *NIM1-INTERACTING 2-like,* we identified five DEGs encoding: two MACPF domain-containing proteins (Solyc01g005220 and Solyc02g077780), the latter being implicated in the negative regulation of the SA-related defense responses (Noutoshi et al., 2006), and three NIM1-like proteins (Solyc07g040690, Solyc02g069310 and Solyc07g044980) (Figure 3a). All of these genes were upregulated in the presence of root pathogens, whereas their expression pattern were more variable in response to the leaf parasite *M. euphorbiae*. We, then, identified six candidates associated with auxin response, including two members of the small auxin upregulated RNA (SAUR) family (Solyc01g110907 and Solyc07g042470), known to regulate cell elongation and the activation of plasma membrane H^+-ATPases (Spartz et al., 2016) (Figure 3b). Finally, we identified 11 DEGs associated to ethylene response in the three interactions, which held the attention given the pivotal role of ethylene in term of regulation of plant development and stress resilience (Figure 3c). Among these DEGs, we detected several transcription factor encoding genes, including *Solyc05g052050,* which encodes Pti4, a protein interacting with the resistance Pto kinase protein and cis regulatory elements (Zhou et al., 1997) and *Solyc06g053710,* which encodes the ethylene receptor ETR4 (Figure 3c). Using the Plant Transcription Factor Database (Tian et al., 2019), we further identified 34 up-regulated (Figure 3d) and 92 down-regulated (Figure 3e) genes across the three interactions within the "*Solanum lycopersicum* Transcription Factors database", covering 29 transcription factor families. The representations between TF families differ between up- and down- regulated candidates. Up-regulated genes in all three interactions showed a top enrichment within the ERF and WRKY families (Figure 3d), whereas down-regulated candidates displayed the bHLH and MYB-related families as top enrichments (Figure 3e). We then assessed whether the putative hubs identified by transcriptomics in *S. lycopersicum* might have *A. thaliana* homologs encoding characterized effector hubs, *i.e.* host proteins interacting with several pathogen effectors. We identified orthologs/homologs between *S. lycopersicum* and *A. thaliana* using OrthoFinder (Emms and Kelly, 2019) and search the EffectorK database compiling *A. thaliana* proteins interacting with pathogen effectors (González-Fuente et al., 2020). Among the *S. lycopersicum* orthologs/homologs of *A. thaliana* effector interactors, we identified, among others, candidate hubs encoding WRKYs (*Solyc03g095770* and *Solyc03g116890*), bHLH (*Solyc05g009880*) and TCP (*Solyc01g008230*) transcription factors, a protein phosphatase 2C (PP2CA) (Solyc03g096670), a protein homologous to RESPONSE TO LOW SULFUR 2 (LSU2) (*Solyc03g096780*) and several paralogs of plasma membrane intrinsic proteins (*Solyc06g011350*, *Solyc09g007760* and *Solyc09g007770*) (Figure 3f). Altogether, these results pointed out a short panel of putative key tomato hubs that could be directly or indirectly affected by at least these three pathogens and acting at multiple levels to promote parasitic success.

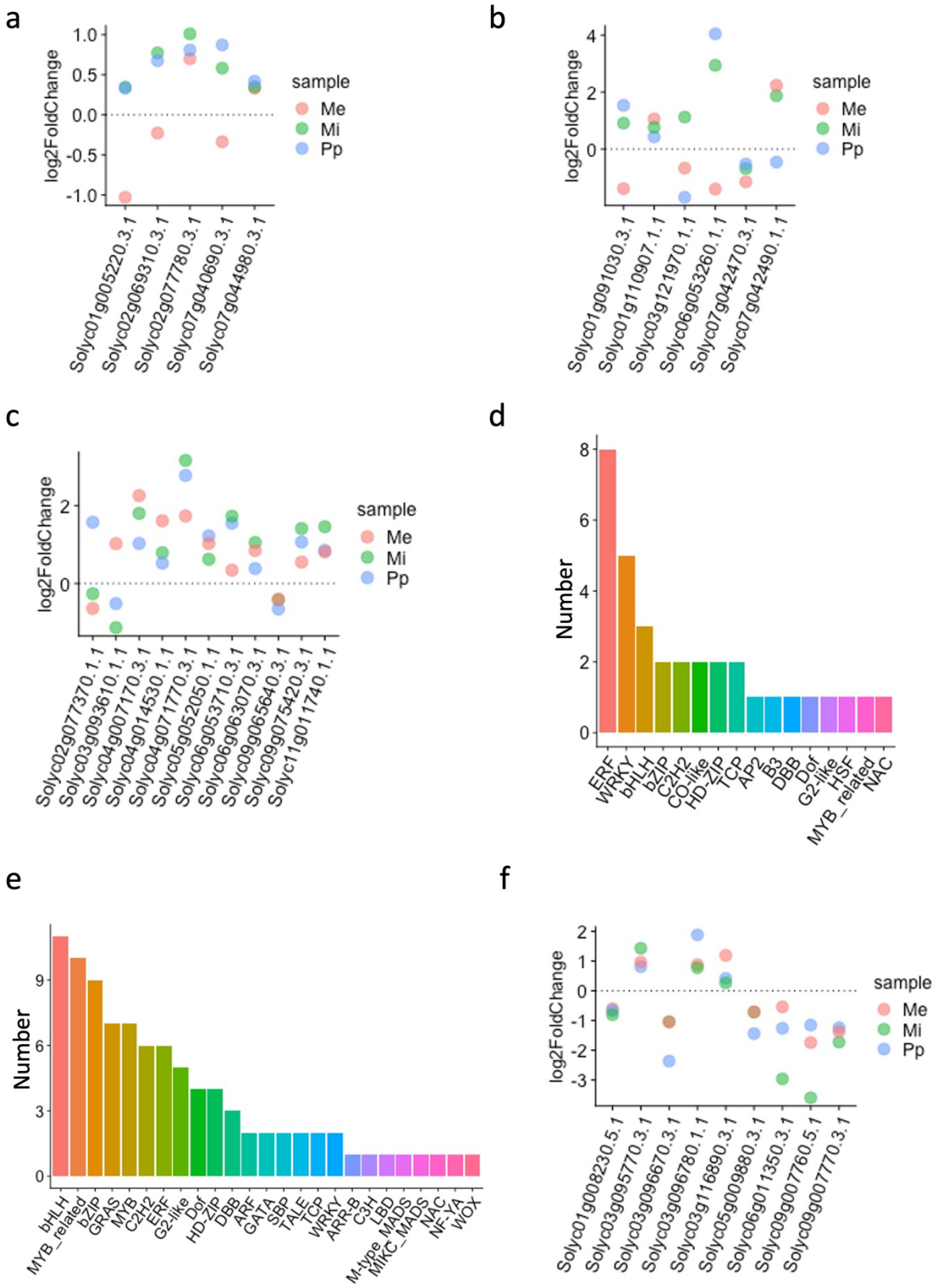

Figure 3 - Characterization of candidate genes with a common response in the three interactions. a. DEGs associated with salicylic acid pathways in the three interactions tested. b. DEGs associated with auxin response in the three interactions tested. c. DEGs associated with ethylene response in the three interactions tested. d. Distribution of candidate genes identified in Plant Transcription Factor Database and

318 up-regulated in the three interactions tested. e. Distribution of candidate genes
319 identified in Plant Transcription Factor Database and down-regulated in the three
320 interactions tested. f. Selection of candidate hubs in *S. lycopersicum* encoding for
321 orthologs of effector interactors in *A. thaliana*. Me: *M. euphorbiae*, Mi: *M. incognita*
322 and Pp: *P. parasitica*

323 **Root and leaf parasites trigger preferentially different pathways**

324 To dissect the regulatory networks underlying parasitic success, we performed a co-expression
325 analysis. We took advantage of publicly available RNA-seq generated from *S. lycopersicum* leaves
326 in presence (24 hpi) or absence of the South American tomato pinworm *Tuta absoluta* (Roumani
327 et al., 2022) to further explore tissue-dependent co-expression patterns. PCA revealed a clear
328 separation between leaves and roots along the first component, accounting for more than 45% of
329 the variance (Figure S4a), consistent with the distinct gene expression patterns observed in roots
330 and leaves (Attard et al., 2010; Pirona et al., 2023). Therefore, we examined the co-expression
331 profiles for root and leaf infections separately using DiCoExpress (Lambert et al., 2020), taking into
332 account the interaction effect between biological factors to identify the genes displaying a common
333 response to the pathogens tested. Multifactorial analysis of the RNA-seq data from the root
334 pathogen experiments (*M. incognita* and *P. parasitica*) pointed out 2,119 candidate genes showing
335 a common response to root pathogens (Figure 4a).
336 Co-expression analysis of these candidates resulted in five clusters (Figure 4b and Figure S4b).
337 Clusters 1, 2 and 3 contained genes generally up-regulated in response to both root pathogens (*M.*
338 *incognita* and *P. parasitica*), whereas clusters 4 and 5 were characterized by a general pattern of
339 downregulation in response to root pathogens. We identified over-represented cluster-specific
340 biological processes using a GO enrichment analysis for each cluster (Figure 4c). Cluster 1 was
341 characterized by an overrepresentation of processes linked with the regulation of SAR and
342 ethylene-activated signaling pathway, including the candidate hub NIM1-INTERACTING 2-like
343 (*Solyc04g007140*) (Figure 1f). In contrast, clusters 2 and 3 showed an enrichment in processes
344 associated with programmed cell death (PCD) and regulation of jasmonic acid mediated signaling
345 pathway (including the NIM1-like protein 1 encoded by *Solyc02g069310*) (Figure 3a). Both clusters
346 were also enriched for GO term “regulation of SA mediated signaling pathway”. Processes linked
347 to trehalose biosynthetic process and response to hormone were overrepresented in clusters 4 and
348 5, respectively (Figure 4c). Notably, clusters 3 and 4 shared an enrichment in processes linked to
349 protein phosphorylation despite displaying opposite co-expression patterns. This suggests that
350 genes belonging to the same pathway may have opposite roles (positive /negative regulators), and
351 that parasites may need to up-regulate some components while downregulating others to achieve
352 parasitic success (Figure 4c).

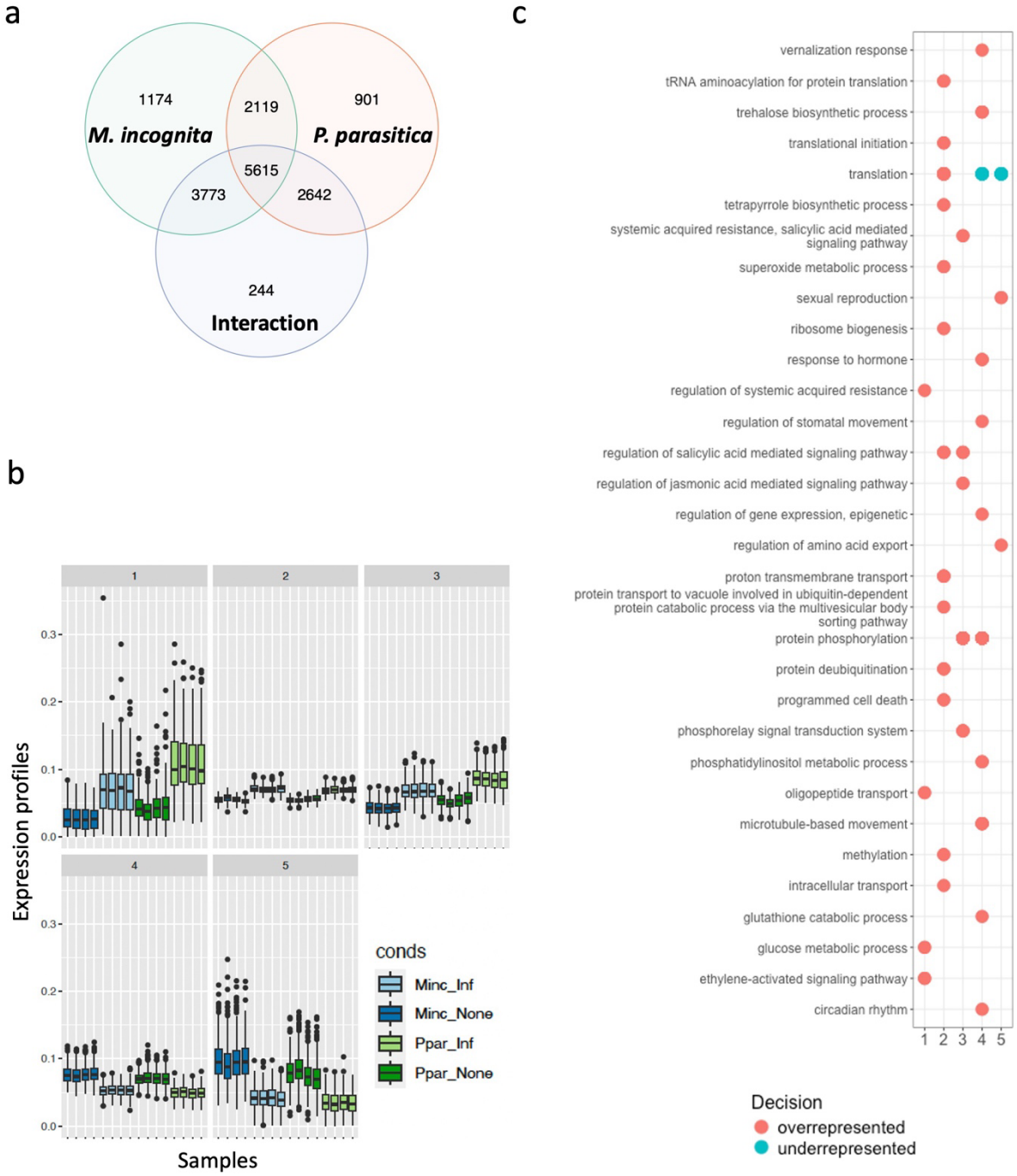

Figure 4 - Co-expression analysis of root response to telluric parasites. (a) Venn diagram of DEGs in roots in response to *M. incognita*, *P. parasitica* taking into account the interaction of both factors. (b) Co-expression showing the five clusters with boxplot expression profiles per sample per conditions. (c) GO enrichment of biological processes for the five co-expression clusters containing gene candidates commonly dysregulated in presence of root pathogens.

362 We then performed a similar analysis with leaf pathogens (*M. euphorbiae* and *T. absoluta*).
363 Multifactorial analysis identified 938 genes showing a common response to leaf pathogens (Figure
364 5a). Co-expression analysis of these candidates also resulted in five clusters (Figure 5b and Figure
365 S4c). As observed with root pathogens, GO enrichments were cluster specific (Figure 5c). Cluster
366 1 showed an overrepresentation of processes related to vesicle trafficking and carbohydrate
367 metabolic process, with candidates associated with cell wall remodeling such as the beta-
368 mannosidase (*Solyc03g119080*) (Pirona et al., 2023). Additional cell wall-associated genes, such
369 as *Solyc09g098510* (extensin-2-like), were present in cluster 2, which was enriched in plant-type
370 cell wall organization processes. Cluster 3 displayed enrichments in processes associated with
371 protein phosphorylation and photosynthesis. Among the genes in cluster 3, the MAP kinase kinase
372 kinase encoding gene *Solyc02g065110* has been associated with the induction of PCD (Roberts
373 et al., 2019). Cluster 4 was enriched in ion transport processes with cyclic nucleotide-gated ion
374 channel candidates, consistent with the changes in ion fluxes associated with plant immune
375 response to pathogens (Moeder et al., 2011) and in hydrogen peroxide catabolic process. Finally,
376 cluster 5 was enriched in inositol catabolism with downregulated inositol oxygenases, a gene family
377 involved in the cell wall biosynthesis and ascorbic acid biosynthesis pathway (Munir et al., 2020).
378 Although several candidate genes responded to both root and leaf pathogens, the co-expression
379 analyses revealed a panel of biological processes significantly over-represented in a cluster and
380 tissue specific manner. These results unveiled clear distinct modules of underlying regulations
381 associated with pathogen responses.

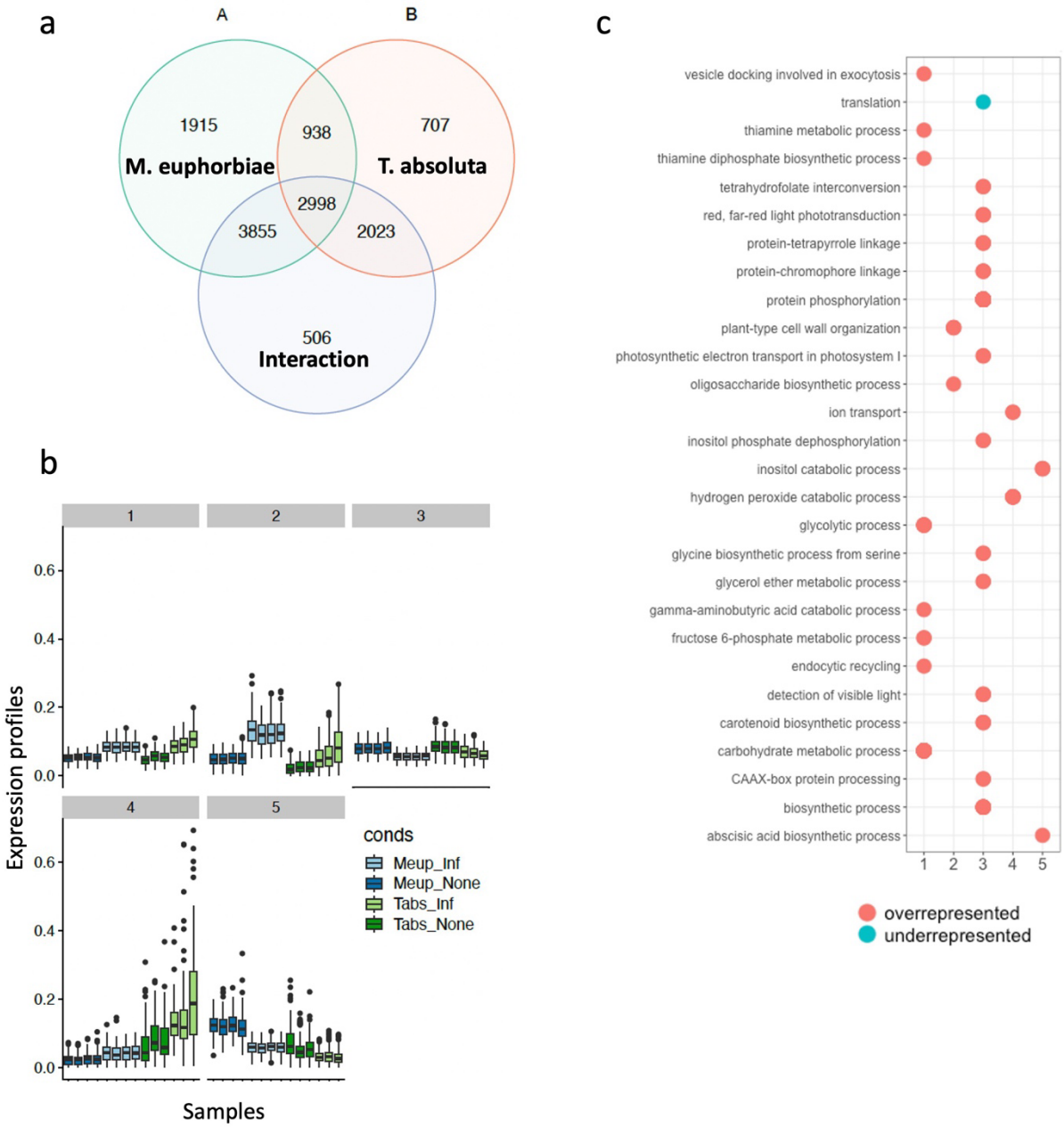

Figure 5 - (a) Venn diagram of DEG in leaf in response to *M. euphorbiae* and *T. absoluta* taking into account the interaction of both factors. (b) Co-expression clusters with the boxplot expression profiles per sample per conditions in leaves. (c) GO enrichment of biological processes per co-expression cluster gene candidates commonly dysregulated in presence of leaf pathogens.

391 **Putative *S.* lycopersicum hubs targeted by parasites are homologs of *A. thaliana* hubs**

392 Finally, we evaluated the relevance of our candidate hubs within the experimentally tested *A.*
393 *thaliana* interactome network in a model-to-crop translational work using OrthoFinder-identified
394 orthologs as proxies. We characterized over 900 homologs of the putative hubs identified in this
395 study within the *A. thaliana* interactome network, most of which taking part in complex, highly
396 interconnected networks (in orange in Figure 6a). To reconstruct the networks affected by the three
397 parasites, we then considered only the interactions between the homologs of our candidate hubs.
398 This analysis revealed the central positions of several effector-interacting homologs, such as the
399 PP2CA (Solyc03g096670 ortholog) and the plasma membrane intrinsic protein PIP2A (associated
400 with paralogs Solyc06g011350, Solyc09g007760 and Solyc09g007770), among numerous other
401 candidates (orange nodes in Figure 6b). Furthermore, the analysis pinpointed the pivotal position
402 of NATA1 (AT2G39030, Solyc08g006765 homolog) (in red in Figure 6c). NATA1 interacts with two
403 transcription factors, HB-12 (Solyc01g096320 homolog) and TCP2 (Solyc08g048370 homolog),
404 thereby bridging two important regulatory network subsets. ATHB12 acts as positive transcriptional
405 regulators of *PP2C* genes, and thus as a negative regulator of ABA signaling (Valdés et al., 2012).
406 On the other branch of this network, we identified three TCP transcription factors, TCP2, TCP21
407 and TCP24, which centralize interactions involving numerous DEGs identified in our study. TCP2
408 and TCP21 are known to be directly targeted by pathogen's effectors (González-Fuente et al.,
409 2020; Drcelic et al., 2024; Fu et al., 2025). Consistently, in our study, Solyc08g048370 and
410 Solyc01g008230, the tomato homologs of TCP2 and TCP21, were similarly dysregulated in
411 response to the three parasites, making them strong candidate hubs (Figure S5).

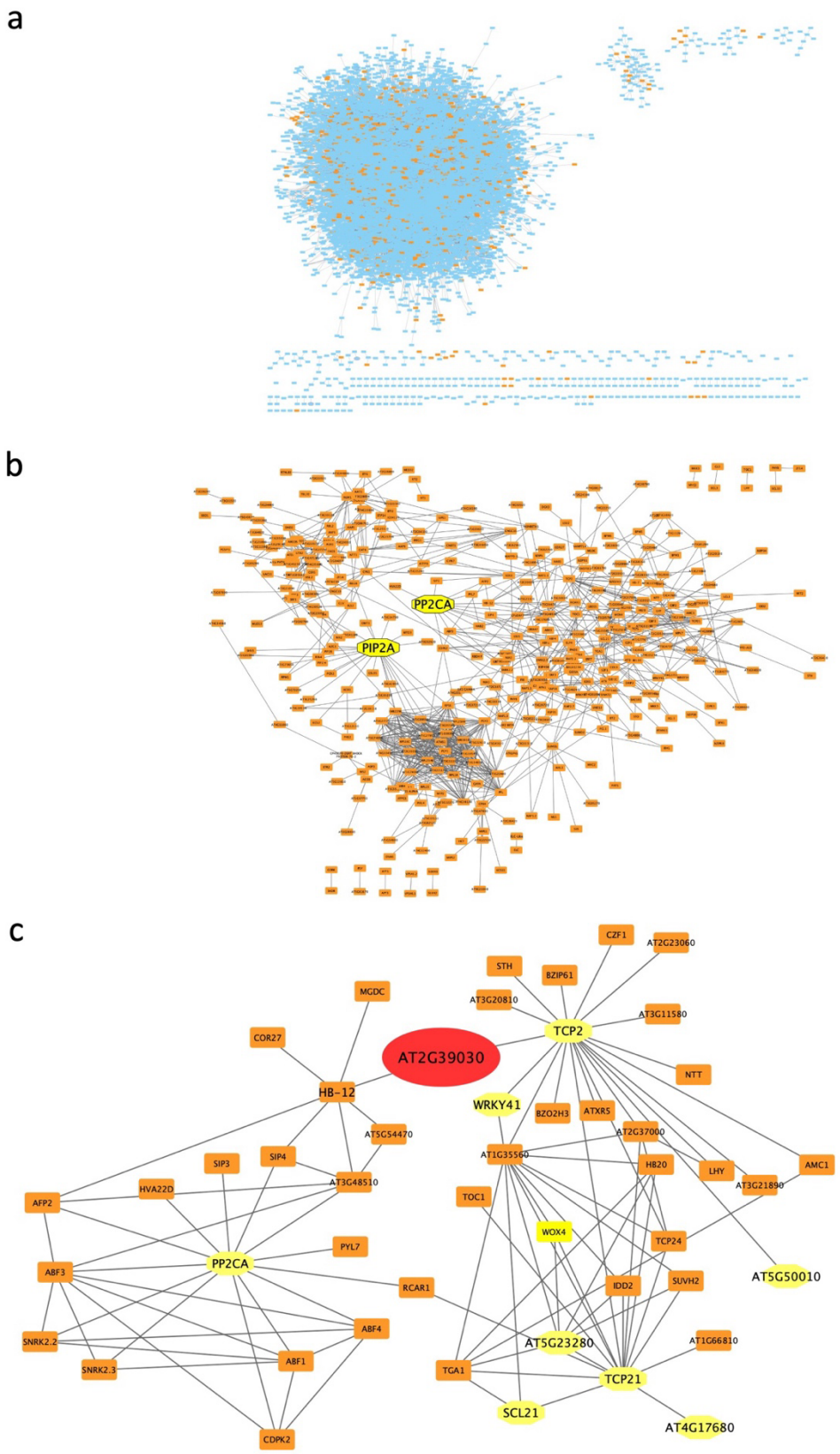

Figure 6 - S. lycopersicum orthologs in the context of experimentally tested A. thaliana regulatory network. In orange, the orthologs/homologs of candidate hubs identified in S. lycopersicum (this study). (a) A. thaliana full interactome network highlighting, the orthologs/homologs of candidate hubs identified in S. lycopersicum

(this study). (b) A. thaliana interactome subset showing only the interactions between the orthologs/homologs of candidate hubs identified in this study. (c) A. thaliana interactome subset highlighting the key position of NATA1 (AT2G39030 in red) among the network of orthologs/homologs of candidate hubs. In yellow: effector interacting proteins.

Discussion

Compatible plant-pathogen interactions rely on the pathogens ability to manipulate host gene expression in order to (1) facilitate pathogen entry through interference with the integrity of physical barriers such as modulations of the cell wall structure or stomatal opening, (2) suppress host immune responses by altering gene expression regulation and hormonal signaling pathways and (3) promote pathogen access to host nutrients via the regulation of metabolite synthesis and nutrient transport (van Schie & Takken, 2014; D. Wang et al., 2025). Such genes can be evolutionary conserved across species (Koseoglou et al., 2022) and may be targeted, directly or indirectly, by effectors from trans-kingdom pathogens. Understanding these hub targets in depth could therefore contribute to the development of broad-spectrum resistance through their targeted impairment.

Although pathogens generally downregulate defense pathways while activating processes that favor their own growth, host responses reflect complex regulatory networks with redundancy and feedback loops, complicating transcriptomic interpretation. Illustrating this conundrum, we found that *Solyc08g080670* was among the most strongly upregulated genes in response to all three parasites tested. This gene is the tomato homolog of *OSM34* in *A. thaliana,* a stress-responsive gene, functioning in the ABA signaling pathway, and potentially playing a role in plant protection against fungi infections (Mukherjee et al., 2010; Hao et al., 2015; Park & Kim, 2021). A recent study demonstrated that the TuMV hijacked *AtOSM34* to promote viral infection. Indeed, *AtOSM34* upregulation reduces plasmodesmata callose deposition to promote viral intercellular movement and targeted viral replication complex to promote viral replication. Additionally, it suppressed the ROS-mediated antiviral response (He et al., 2025). Whether multiple pathogens trigger the upregulation of *Solyc08g080670* to promote infection remains to be determined, but this possibility highlights its potential importance as a key factor to target. Another set of key candidate genes identified in this study are *SlDMR6-1* and *SlDMR6-2,* the closest homologs of the salicylic Acid 5-Hydroxylase DMR6 and DLO, which are well-known susceptibility factors to oomycetes and bacteria. In Arabidopsis, these enzymes function redundantly, in different tissues, to suppress plant immunity. They catalyze the formation of 2,5-Dihydroxybenzoic acid2 (5-DHBA) by hydroxylating SA, thereby inactivating SA (Zeilmaker et al., 2015; van Butselaar et al., 2024). Here, we showed that both genes are strongly overexpressed in tomato in response to all three pathogens tested. Interestingly, *SlDMR6-1* is only slightly induced in response to aphids, consistent with the variable spatial expression mentioned in the literature and with the possibility that *SlDMR6-1* and SlDMR6-2 respond differently depending on the pathogen. For instance, Thomazella et al. (2021) reported an upregulation of *SlDMR6-1* whereas SlDMR6-2 expression was not detected upon infection by *Xanthomonas gardneri* (Thomazella et al., 2021). Although such genes represent potential targets for gene inactivation to enhance plant resistance, their role in maintaining SA homeostasis highlights the trade-off between immunity and growth.

Another important multi-pathogen target identified in our study is the *NIMIN-2* homolog (Solyc04g007140). NIMIN proteins interact with NPR1, the key positive regulator of SAR acting in the SA-mediating pathway (Zavaliev et al., 2020). Interestingly, NIMIN proteins act as negative regulators of NPR1, therefore, the upregulation of *Solyc04g007140* is likely to favor pathogen

infection by compromising SAR, making it a prominent target (Weigel et al., 2005). Pathogen infections also affected host epigenetic factors. Indeed, *Solyc06g066420* belongs to the *OXS 3* family, which, like OSM34, functions in ABA signaling and acts as a chromatin-associated factor involved in tolerance to heavy metals and oxidative stress (Blanvillain et al., 2009). *AtOXS3* has been associated with the regulation of gene expression via modulation of histone γ-H2A.X occupancy (Xiao et al., 2021). *Solyc06g066420* was consistently upregulated across all interactions and is therefore likely to modulate a wide range of gene expression programs. Conversely, *Solyc05g052950*, *AtTCF1* ortholog, was strongly downregulated. AtTCF1 has been studied in the context of abiotic stress, particularly cold acclimatation (Ji et al., 2015). TCF1 indirectly affects lignin accumulation though its association with chromatin at specific loci. Interestingly, loss of TCF1 modified H3K4me2 and H3K27me3 levels, resulting in reduced lignin content (Ji et al., 2015). Because lignin-based barrier restricts pathogen spread and contributes to plant resistance (Lee et al., 2019), *Solyc05g052950* is therefore an excellent epigenetic factor to target, acting upstream lignin accumulation. Together, these findings underscore the importance of chromatin-level regulation during parasitism. Furthermore,
several candidate hubs identified here are also associated with abiotic stress responses (Pirona et al., 2023) reflecting conserved physiological responses—such as ABA signaling, lignin deposition, and stomatal regulation—between biotic and abiotic stress adaptation. This overlap highlights the potential cost of manipulating such hubs for resistance breeding.
Besides, subtilases are involved in a broad range of biological functions including plant defense responses or in plant-pathogen interactions (Weng et al., 2014; Serrano et al., 2016; Stegmann et al., 2017; J. Figueiredo et al., 2018; Zhang et al., 2024). Within this large gene family (around one hundred in *S. lycopersicum*), we identified two genes that were strongly upregulated in response to all three pathogens, while 65 tomato subtilase encoding genes were differentially expressed in response to at least one of them. This result suggests that subtilases are primarily involved in pathogen-specific plant responses. In *S. lycopersicum*, research has mainly focused on the subtilase cluster encoding the P69 proteases, which has been linked to pathogenesis (Jordá et al., 1999; Zhang et al., 2024). For instance, *Pseudomonas syringae* and *Ralstonia solanacearum* infections have been associated with the induction of *P69B* among others (Jordá et al., 1999; Zhang et al., 2024). In our study, *P69B* (*Solyc08g079870*) was also up-regulated in response to *M. incognita*, *P. parasitica* and *M. euphorbiae*. In contrast, little is known about the role of the subtilases of the cluster 1, highlighting an important avenue for future studies to determine their role in pathogenesis.
SA-activated responses are effective against biotrophic pathogens, which retrieve nutrients from living plant cells. In contrast, JA and ET elicit responses that combat necrotrophic microbes, which kill plant cells and feed on the resulting tissues. While activation of the JA pathway suppresses SA biosynthesis and vice versa (Zheng et al., 2012), SA signaling also interferes with JA-ET pathways. For example, SA affects JA-induced transcription by inducing the degradation of transcription factors that activate JA signaling, as shown for the ERF transcription factor ORA59. Additionally, SA can induce negative regulators, among them several WRKY transcription factors, that directly or indirectly inhibit JA-responsive gene expression (Zheng et al., 2012). More than one hundred transcription factors were commonly dysregulated in response to the three pathogens tested. We observed a divergence in the TF family enrichments between the up and down regulated candidates. Similar results were also observed in transcriptomic analysis of *S. lycopersicum* in response to osmotic stress (Pirona et al., 2023). Interestingly, our results and those of (Pirona et al., 2023) showed that, in response to both biotic and abiotic stresses, ERF and bHLH families of transcription factors were among the top enrichment in up and down regulated candidates, respectively, with several common candidate genes responding to both types of stresses.
GO enrichment analyses revealed common overrepresentation of metabolic processes across nematode, aphid, and oomycete infections, supporting the view that parasites enhance host

514 metabolic activity. Beyond a set of commonly dysregulated candidate hubs, roots and leaves
515 diverged markedly in the significantly overrepresented processes identified across the different co-
516 expression clusters. These findings, along with previous studies reporting tissue-specific responses
517 between leaves and roots (Hermanns et al., 2003; Attard et al., 2010), indicate that combining
518 organ-specific with common hubs may be a more effective strategy for engineering broad-spectrum
519 resistance, potentially through rootstock–scion approaches.
520 Finally, we identified *Solyc08g006765*, the tomato homolog of *AtNATA1*, as a central multi-
521 pathogen hub. Insect feeding and *P. syringae* inoculation both upregulate NATA1, leading to the
522 production of N^{δ}-acetylornithine via the jasmonate pathway (Adio et al., 2011). While this metabolite
523 affects the reproduction of the aphid, *Myzus persicae*, *P. syringae* growth was impaired in *nata1*
524 mutant. In addition to jasmonic acid, the coronatine effector produced by DC3000 *P. syringae* strain
525 also induces *NATA1* expression (Lou et al., 2016). Via the acetylation of putrescine, a precursor
526 required for the defense-related hydrogen peroxide, NATA1 acts as a susceptibility factor
527 competing for this common substrate impeding plant defense response (Lou et al., 2016).
528 Furthermore, we noted that several NATA1 interactors, including TCP transcription factors, are also
529 direct targets of known effectors (González-Fuente et al., 2020; Drcelic et al., 2024; Fu et al., 2025).
530 We identified tomato homologs of AtTCP2 and AtTCP21 as consistently dysregulated in presence
531 of all three pathogens. Although *SlTCP2* and *SlTCP21* belong to different classes and are probably
532 involved in two different pathways, their expression is clearly affected by multiple pathogens.
533 Additionally, TCP21, also named CHE for CCA1 Hiking Expedition, was recently described to be
534 the missing link between local infection and the SAR making it a compelling hub (Cao et al., 2024).
535 We propose that these transcription factors and especially *TCP21* (*CHE*), should be considered as
536 a key regulatory hub in future studies of tomato pathogen interactions.
537 Far beyond the trivial production of a repertoire of commonly dysregulated genes, we implemented
538 an in-depth co-expression analysis that pinpoint compelling candidate hubs covering a large range
539 of functions and pathways. By pairing our results obtained in tomato with Arabidopsis interactome
540 network data, we found crucial factors associated with parasitic success that should be of interest
541 for plant breeding programs.

542 Acknowledgments

543 The authors are grateful to Marie-Laure Martin and Etienne Delannoy (IPS2, Orsay, France) for
544 their guidance with the co-expression analysis and Romain Larbat (IRHS, Angers, France) for
545 sharing the RNA-seq datasets of tomato response to *T. absoluta* (Roumani et al., 2022). The
546 authors thank the bioinformatics and genomics platform BIG (ISA, Sophia Antipolis, France,
547 plantBIOs, https://doi.org/10.15454/qyey-ar89) for computing and storage resources and the
548 Genotoul bioinformatics platform (Bioinfo Genotoul, Toulouse, France
549 https://doi.org/10.15454/1.5572369328961167E12) for computing resources.

550 Data, scripts, code, and supplementary information availability

551 The datasets generated for this study are available under the BioProject PRJNA1375716. The
552 datasets of tomato response to *T. absoluta* infection at 24 hpi (Roumani et al., 2022) were retrieved
553 through the accession number GSE200795. Supplementary information and code are available at
554 https://doi.org/10.57745/GL5MLM, https://forge.inrae.fr/GNet/dicoexpress/-
555 /tree/985351e4e49c854f1bcb894de585c6939374f8bc/ and
556 https://forge.inrae.fr/plantbios_big/nextflow/mapping_count_featurecount_rsem/-
557 /tree/f9f4b7dd59fb5cc295c446ab9fd067a41956071c/.

558 ## Conflict of interest disclosure

559 The authors declare that they have no financial conflicts of interest in relation to the content of the
560 article.

561 ## Funding

562 This work was funded by the Plant Health and Environment (SPE) division from INRAE (2021-2023
563 TRIP project) and the CSI-2021 IDEX (2021 ICARE project). BF is supported by INRAE and the
564 French Government (National Research Agency, ANR) through the "Investments for the Future"
565 LabEx SIGNALIFE (#ANR-11-LABX-0028-01) and the MASH project (#ANR-21-CE20-0002).

566 ## References

567 Abad P, Gouzy J, Aury JM, Castagnone-Sereno P, Danchin EG, Deleury E, Perfus-Barbeoch L,
568 Anthouard V, Artiguenave F, Blok VC, Caillaud MC, Coutinho PM, Dasilva C, De Luca F, Deau F,
569 Esquibet M, Flutre T, Goldstone JV, Hamamouch N, Hewezi T, Jaillon O, Jubin C, Leonetti P,
570 Magliano M, Maier TR, Markov GV, McVeigh P, Pesole G, Poulain J, Robinson-Rechavi M, Sallet E,
571 Segurens B, Steinbach D, Tytgat T, Ugarte E, van Ghelder C, Veronico P, Baum TJ, Blaxter M,
572 Bleve-Zacheo T, Davis EL, Ewbank JJ, Favery B, Grenier E, Henrissat B, Jones JT, Laudet V, Maule
573 AG, Quesneville H, Rosso MN, Schiex T, Smant G, Weissenbach J, Wincker P (2008) Genome
574 sequence of the metazoan plant-parasitic nematode Meloidogyne incognita. *Nat Biotechnol,* **26**, 909-
575 915. https://doi.org/10.1038/nbt.1482

576 Adio AM, Casteel CL, De Vos M, Kim JH, Joshi V, Li B, Juéry C, Daron J, Kliebenstein DJ, Jander G
577 (2011) Biosynthesis and defensive function of N δ-acetylornithine, a jasmonate-induced Arabidopsis
578 metabolite. *The Plant Cell,* **23**, 3303-3318. https://doi.org/10.1105/tpc.111.088989

579 Attard A, Gourgues M, Callemeyn-Torre N, Keller H (2010) The immediate activation of defense
580 responses in Arabidopsis roots is not sufficient to prevent Phytophthora parasitica infection. *New*
581 *Phytologist,* **187**, 449-460. https://doi.org/10.1111/j.1469-8137.2010.03272.x

582 Attard A, Gourgues M, Galiana E, Panabieres F, Ponchet M, Keller H (2008) Strategies of attack and
583 defense in plant–oomycete interactions, accentuated for Phytophthora parasitica Dastur (syn. P.
584 Nicotianae Breda de Haan). *Journal of Plant Physiology,* **165**, 83-94.
585 https://doi.org/10.1016/j.jplph.2007.06.011

586 Biniaz Y, Tahmasebi A, Tahmasebi A, Albrectsen BR, Poczai P, Afsharifar A (2022) Transcriptome
587 meta-analysis identifies candidate hub genes and pathways of pathogen stress responses in
588 Arabidopsis thaliana. *Biology,* **11**, 1155. https://doi.org/10.3390/biology11081155

589 Blanvillain R, Kim JH, Wu S, Lima A, Ow DW (2009) OXIDATIVE STRESS 3 is a chromatin-associated
590 factor involved in tolerance to heavy metals and oxidative stress. *The Plant Journal,* **57**, 654-665.
591 https://doi.org/10.1111/j.1365-313X.2008.03717.x

592 Blok VC, Jones JT, Phillips MS, Trudgill DL (2008) Parasitism genes and host range disparities in
593 biotrophic nematodes: the conundrum of polyphagy versus specialisation. *BioEssays,* **30**, 249-259.
594 https://doi.org/10.1002/bies.20717

595 Campos MD, Félix MdR, Patanita M, Materatski P, Varanda C (2021) High throughput sequencing
596 unravels tomato-pathogen interactions towards a sustainable plant breeding. *Horticulture Research,*
597 **8**, 171. https://doi.org/10.1038/s41438-021-00607-x
598 Cao L, Karapetyan S, Yoo H, Chen T, Mwimba M, Zhang X, Dong X (2024) H2O2 sulfenylates CHE,
599 linking local infection to the establishment of systemic acquired resistance. *Science,* **385**, 1211-1217.
600 https://doi.org/10.1126/science.adj7249
601 Carella P, Evangelisti E, Schornack S (2018) Sticking to it: phytopathogen effector molecules may
602 converge on evolutionarily conserved host targets in green plants. *Current opinion in plant biology,*
603 **44**, 175-180. https://doi.org/10.1016/j.pbi.2018.04.019
604 Coppola V, Coppola M, Rocco M, Digilio MC, D'Ambrosio C, Renzone G, Martinelli R, Scaloni A,
605 Pennacchio F, Rao R (2013) Transcriptomic and proteomic analysis of a compatible tomato-aphid
606 interaction reveals a predominant salicylic acid-dependent plant response. *BMC genomics,* **14**, 515.
607 https://doi.org/10.1186/1471-2164-14-515
608 Drcelic M, Skiljaica A, Polak B, Bauer N, Seruga Music M (2024) 'Candidatus Phytoplasma
609 solani'Predicted Effector SAP11-like Alters Morphology of Transformed Arabidopsis Plants and
610 Interacts with AtTCP2 and AtTCP4 Plant Transcription Factors. *Pathogens,* **13**, 893.
611 https://doi.org/10.3390/pathogens13100893
612 Favery B, Dubreuil G, Chen M-S, Giron D, Abad P (2020) Gall-inducing parasites: convergent and
613 conserved strategies of plant manipulation by insects and nematodes. *Annual Review of*
614 *Phytopathology,* **58**, 1-22. https://doi.org/10.1146/annurev-phyto-010820-012722
615 Figueiredo A, Monteiro F, Sebastiana M (2014) Subtilisin-like proteases in plant-pathogen recognition
616 and immune priming: a perspective. *Front Plant Sci,* **5**, 739. https://doi.org/10.3389/fpls.2014.00739
617 Figueiredo J, Sousa Silva M, Figueiredo A (2018) Subtilisin-like proteases in plant defence: the past,
618 the present and beyond. *Mol Plant Pathol,* **19**, 1017-1028. https://doi.org/10.1111/mpp.12567
619 Fu M, Zhou Y, Zhang X, Yang K, Xu Y, Wang X, Chen Z, Wang Y, Shi Y, Ma L (2025) A pathogen
620 effector HaRxL10 hijacks the circadian clock component CHE to perturb both plant development and
621 immunity. *Nature Communications,* **16**, 1538. https://doi.org/10.1038/s41467-025-56787-w
622 González-Fuente M, Carrère S, Monachello D, Marsella BG, Cazalé AC, Zischek C, Mitra RM, Rezé N,
623 Cottret L, Mukhtar MS, Lurin C, Noël LD, Peeters N (2020) EffectorK, a comprehensive resource to
624 mine for Ralstonia, Xanthomonas, and other published effector interactors in the Arabidopsis
625 proteome. *Mol Plant Pathol,* **21**, 1257-1270. https://doi.org/10.1111/mpp.12965
626 Hao J, Wu W, Wang Y, Yang Z, Liu Y, Lv Y, Zhai Y, Yang J, Liang Z, Huang K (2015) Arabidopsis
627 thaliana defense response to the ochratoxin A-producing strain (Aspergillus ochraceus 3.4412). *Plant*
628 *Cell Reports,* **34**, 705-719. https://doi.org/10.1007/s00299-014-1731-3
629 He R, Li Y, Bernards MA, Wang A (2025) Turnip mosaic virus selectively subverts a PR-5 thaumatin-
630 like, plasmodesmal protein to promote viral infection. *New Phytologist,* **245**, 299-317.
631 https://doi.org/10.1111/nph.20233
632 Hermanns M, Slusarenko AJ, Schlaich NL (2003) Organ-specificity in a plant disease is determined
633 independently of R gene signaling. *Molecular Plant-Microbe Interactions,* **16**, 752-759.
634 https://doi.org/10.1094/MPMI.2003.16.9.752

635 Jaouannet M, Morris JA, Hedley PE, Bos JI (2015) Characterization of Arabidopsis transcriptional
636 responses to different aphid species reveals genes that contribute to host susceptibility and non-host
637 resistance. *PLoS pathogens,* **11**, e1004918. https://doi.org/10.1371/journal.ppat.1004918
638 Ji H, Wang Y, Cloix C, Li K, Jenkins GI, Wang S, Shang Z, Shi Y, Yang S, Li X (2015) The Arabidopsis
639 RCC1 family protein TCF1 regulates freezing tolerance and cold acclimation through modulating
640 lignin biosynthesis. *PLoS genetics,* **11**, e1005471. https://doi.org/10.1371/journal.pgen.1005471.
641 eCollection 2015
642 Jones JD, Dangl JL (2006) The plant immune system. *Nature,* **444**, 323-329.
643 https://doi.org/10.1038/nature05286
644 Jordá L, Coego A, Conejero V, Vera P (1999) A Genomic Cluster Containing Four Differentially
645 Regulated Subtilisin-like Processing Protease Genes Is in Tomato Plants *. *Journal of Biological*
646 *Chemistry,* **274**, 2360-2365. https://doi.org/10.1074/jbc.274.4.2360
647 Kamoun S, Furzer O, Jones JD, Judelson HS, Ali GS, Dalio RJ, Roy SG, Schena L, Zambounis A,
648 Panabières F (2015) The Top 10 oomycete pathogens in molecular plant pathology. *Molecular plant*
649 *pathology,* **16**, 413-434. https://doi.org/10.1111/mpp.12190
650 Kong F, Yang L (2023) Pathogen-triggered changes in plant development: Virulence strategies or host
651 defense mechanism? *Frontiers in Microbiology,* **14**, 1122947.
652 https://doi.org/10.3389/fmicb.2023.1122947
653 Koseoglou E, van der Wolf JM, Visser RGF, Bai Y (2022) Susceptibility reversed: modified plant
654 susceptibility genes for resistance to bacteria. *Trends in Plant Science,* **27**, 69-79.
655 https://doi.org/https://doi.org/10.1016/j.tplants.2021.07.018
656 Lambert I, Paysant-Le Roux C, Colella S, Martin-Magniette ML (2020) DiCoExpress: a tool to process
657 multifactorial RNAseq experiments from quality controls to co-expression analysis through differential
658 analysis based on contrasts inside GLM models. *Plant Methods,* **16**, 68.
659 https://doi.org/10.1186/s13007-020-00611-7
660 Lee MH, Jeon HS, Kim SH, Chung JH, Roppolo D, Lee HJ, Cho HJ, Tobimatsu Y, Ralph J, Park OK
661 (2019) Lignin-based barrier restricts pathogens to the infection site and confers resistance in plants.
662 *The EMBO journal,* **38**, e101948. https://doi.org/10.15252/embj.2019101948
663 Lou YR, Bor M, Yan J, Preuss AS, Jander G (2016) Arabidopsis NATA1 Acetylates Putrescine and
664 Decreases Defense-Related Hydrogen Peroxide Accumulation. *Plant Physiol,* **171**, 1443-1455.
665 https://doi.org/10.1104/pp.16.00446
666 Mejias J, Bazin J, Truong N-M, Chen Y, Marteu N, Bouteiller N, Sawa S, Crespi MD, Vaucheret H, Abad
667 P (2021) The root-knot nematode effector MiEFF18 interacts with the plant core spliceosomal protein
668 SmD1 required for giant cell formation. *The New Phytologist,* **229**, 3408-3423.
669 https://doi.org/10.1111/nph.17089
670 Moeder W, Urquhart W, Ung H, Yoshioka K (2011) The Role of Cyclic Nucleotide-Gated Ion Channels
671 in Plant Immunity. *Molecular Plant,* **4**, 442-452. https://doi.org/https://doi.org/10.1093/mp/ssr018
672 Mukherjee AK, Carp M-J, Zuchman R, Ziv T, Horwitz BA, Gepstein S (2010) Proteomics of the response
673 of Arabidopsis thaliana to infection with Alternaria brassicicola. *Journal of proteomics,* **73**, 709-720.
674 https://doi.org/10.1016/j.jprot.2009.10.005

675 Mukhtar MS, Carvunis AR, Dreze M, Epple P, Steinbrenner J, Moore J, Tasan M, Galli M, Hao T,
676 Nishimura MT, Pevzner SJ, Donovan SE, Ghamsari L, Santhanam B, Romero V, Poulin MM,
677 Gebreab F, Gutierrez BJ, Tam S, Monachello D, Boxem M, Harbort CJ, McDonald N, Gai L, Chen
678 H, He Y, Vandenhaute J, Roth FP, Hill DE, Ecker JR, Vidal M, Beynon J, Braun P, Dangl JL (2011)
679 Independently evolved virulence effectors converge onto hubs in a plant immune system network.
680 *Science,* **333**, 596-601. https://doi.org/10.1126/science.1203659
681 Munir S, Mumtaz MA, Ahiakpa JK, Liu G, Chen W, Zhou G, Zheng W, Ye Z, Zhang Y (2020) Genome-
682 wide analysis of Myo-inositol oxygenase gene family in tomato reveals their involvement in ascorbic
683 acid accumulation. *BMC genomics,* **21**, 284. https://doi.org/10.1186/s12864-020-6708-8
684 Naveed ZA, Ali GS (2018) Comparative transcriptome analysis between a resistant and a susceptible
685 wild tomato accession in response to Phytophthora parasitica. *International Journal of Molecular*
686 *Sciences,* **19**, 3735. https://doi.org/10.3390/ijms19123735
687 Noutoshi Y, Kuromori T, Wada T, Hirayama T, Kamiya A, Imura Y, Yasuda M, Nakashita H, Shirasu K,
688 Shinozaki K (2006) Loss of Necrotic Spotted Lesions 1 associates with cell death and defense
689 responses in Arabidopsis thaliana. *Plant Mol Biol,* **62**, 29-42. https://doi.org/10.1007/s11103-006-
690 9001-6
691 Park E-J, Kim T-H (2021) Arabidopsis OSMOTIN 34 functions in the ABA signaling pathway and is
692 regulated by proteolysis. *International Journal of Molecular Sciences,* **22**, 7915.
693 https://doi.org/10.3390/ijms22157915
694 Pirona R, Frugis G, Locatelli F, Mattana M, Genga A, Baldoni E (2023) Transcriptomic analysis reveals
695 the gene regulatory networks involved in leaf and root response to osmotic stress in tomato. *Front*
696 *Plant Sci,* **14**, 1155797. https://doi.org/10.3389/fpls.2023.1155797
697 Reichardt S, Repper D, Tuzhikov AI, Galiullina RA, Planas-Marquès M, Chichkova NV, Vartapetian AB,
698 Stintzi A, Schaller A (2018) The tomato subtilase family includes several cell death-related
699 proteinases with caspase specificity. *Scientific Reports,* **8**, 10531. https://doi.org/10.1038/s41598-
700 018-28769-0
701 Roberts R, Hind SR, Pedley KF, Diner BA, Szarzanowicz MJ, Luciano-Rosario D, Majhi BB, Popov G,
702 Sessa G, Oh C-S (2019) Mai1 protein acts between host recognition of pathogen effectors and
703 mitogen-activated protein kinase signaling. *Molecular Plant-Microbe Interactions,* **32**, 1496-1507.
704 https://doi.org/10.1094/MPMI-05-19-0121-R
705 Roumani M, Le Bot J, Boisbrun M, Magot F, Péré A, Robin C, Hilliou F, Larbat R (2022) Transcriptomics
706 and Metabolomics Analyses Reveal High Induction of the Phenolamide Pathway in Tomato Plants
707 Attacked by the Leafminer Tuta absoluta. *Metabolites,* **12**. https://doi.org/10.3390/metabo12060484
708 Serrano I, Buscaill P, Audran C, Pouzet C, Jauneau A, Rivas S (2016) A non canonical subtilase
709 attenuates the transcriptional activation of defence responses in Arabidopsis thaliana. *eLife,* **5**,
710 e19755. https://doi.org/10.7554/eLife.19755
711 Spartz AK, Lor VS, Ren H, Olszewski NE, Miller ND, Wu G, Spalding EP, Gray WM (2016) Constitutive
712 Expression of Arabidopsis SMALL AUXIN UP RNA19 (SAUR19) in Tomato Confers Auxin-
713 Independent Hypocotyl Elongation. *Plant physiology,* **173**, 1453-1462.
714 https://doi.org/10.1104/pp.16.01514

715 Stegmann M, Monaghan J, Smakowska-Luzan E, Rovenich H, Lehner A, Holton N, Belkhadir Y, Zipfel
716 C (2017) The receptor kinase FER is a RALF-regulated scaffold controlling plant immune signaling.
717 *Science,* **355**, 287-289. https://doi.org/10.1126/science.aal2541
718 Thomazella DPT, Seong K, Mackelprang R, Dahlbeck D, Geng Y, Gill US, Qi T, Pham J, Giuseppe P,
719 Lee CY, Ortega A, Cho MJ, Hutton SF, Staskawicz B (2021) Loss of function of a DMR6 ortholog in
720 tomato confers broad-spectrum disease resistance. *Proc Natl Acad Sci U S A,* **118**.
721 https://doi.org/10.1073/pnas.2026152118
722 Tian F, Yang D-C, Meng Y-Q, Jin J, Gao G (2019) PlantRegMap: charting functional regulatory maps in
723 plants. *Nucleic Acids Research,* **48**, D1104-D1113. https://doi.org/10.1093/nar/gkz1020
724 Valdés AE, Övernäs E, Johansson H, Rada-Iglesias A, Engström P (2012) The homeodomain-leucine
725 zipper (HD-Zip) class I transcription factors ATHB7 and ATHB12 modulate abscisic acid signalling
726 by regulating protein phosphatase 2C and abscisic acid receptor gene activities. *Plant Molecular*
727 *Biology,* **80**, 405-418. https://doi.org/10.1007/s11103-012-9956-4
728 van Butselaar T, Silva S, Lapin D, Bañales I, Tonn S, van Schie C, Van den Ackerveken G (2024) The
729 role of salicylic acid in the expression of RECEPTOR-LIKE PROTEIN 23 and other immunity-related
730 genes. *Phytopathology®,* **114**, 1097-1105. https://doi.org/10.1094/PHYTO-10-23-0413-KC
731 van Schie CC, Takken FL (2014) Susceptibility genes 101: how to be a good host. *Annual Review of*
732 *Phytopathology,* **52**, 551-581. https://doi.org/ 10.1146/annurev-phyto-102313-045854
733 Walling LL (2008) Avoiding effective defenses: strategies employed by phloem-feeding insects. *Plant*
734 *physiology,* **146**, 859-866. https://doi.org/10.1104/pp.107.113142
735 Wang D, Mandal P, Rahman MS, Yang L (2025) Engineering tomato disease resistance by manipulating
736 susceptibility genes. *Frontiers in Genome Editing,* **7**, 1537148.
737 https://doi.org/10.3389/fgeed.2025.1537148
738 Wang F, Park Y-L, Gutensohn M (2021) Epidermis-specific metabolic engineering of sesquiterpene
739 formation in tomato affects the performance of potato aphid Macrosiphum euphorbiae. *Frontiers in*
740 *plant science,* **12**, 793313. https://doi.org/10.3389/fpls.2021.793313
741 Wang Y, Li T, Sun Z, Huang X, Yu N, Tai H, Yang Q (2022) Comparative transcriptome meta-analysis
742 reveals a set of genes involved in the responses to multiple pathogens in maize. *Frontiers in plant*
743 *science,* **13**, 971371. https://doi.org/10.3389/fpls.2022.971371
744 Weigel RR, Pfitzner UM, Gatz C (2005) Interaction of NIMIN1 with NPR1 modulates PR gene expression
745 in Arabidopsis. *The Plant Cell,* **17**, 1279-1291. https://doi.org/10.1105/tpc.104.027441
746 Weng K, Li Z-Q, Liu R-Q, Wang L, Wang Y-J, Xu Y (2014) Transcriptome of Erysiphe necator-infected
747 Vitis pseudoreticulata leaves provides insight into grapevine resistance to powdery mildew.
748 *Horticulture Research,* **1**. https://doi.org/10.1038/hortres.2014.49
749 Xiao S, Jiang L, Wang C, Ow DW (2021) Arabidopsis OXS3 family proteins repress ABA signaling
750 through interactions with AFP1 in the regulation of ABI4 expression. *Journal of Experimental Botany,*
751 **72**, 5721-5734. https://doi.org/ 10.1093/jxb/erab237
752 Zavaliev R, Mohan R, Chen T, Dong X (2020) Formation of NPR1 condensates promotes cell survival
753 during the plant immune response. *Cell,* **182**, 1093-1108. e1018.
754 https://doi.org/10.1016/j.cell.2020.07.016

755 Zeilmaker T, Ludwig NR, Elberse J, Seidl MF, Berke L, Van Doorn A, Schuurink RC, Snel B, Van den
756 Ackerveken G (2015) DOWNY MILDEW RESISTANT 6 and DMR 6-LIKE OXYGENASE 1 are
757 partially redundant but distinct suppressors of immunity in Arabidopsis. *The Plant Journal,* **81**, 210-
758 222. https://doi.org/10.1111/tpj.12719
759 Zhang W, Planas-Marquès M, Mazier M, Šimkovicová M, Rocafort M, Mantz M, Huesgen PF, Takken
760 FLW, Stintzi A, Schaller A, Coll NS, Valls M (2024) The tomato P69 subtilase family is involved in
761 resistance to bacterial wilt. *Plant J,* **118**, 388-404. https://doi.org/10.1111/tpj.16613
762 Zheng XY, Spivey NW, Zeng W, Liu PP, Fu ZQ, Klessig DF, He SY, Dong X (2012) Coronatine promotes
763 Pseudomonas syringae virulence in plants by activating a signaling cascade that inhibits salicylic
764 acid accumulation. *Cell Host Microbe,* **11**, 587-596. https://doi.org/10.1016/j.chom.2012.04.014
765 Zhou J, Tang X, Martin GB (1997) The Pto kinase conferring resistance to tomato bacterial speck
766 disease interacts with proteins that bind a cis-element of pathogenesis-related genes. *Embo j,* **16**,
767 3207-3218. https://doi.org/10.1093/emboj/16.11.3207
768